Phase equilibria in systems of hard disks with thickness polydispersity

H. H. Wensink and G. J. Vroege*
Van't Hoff Laboratory for Physical and Colloid Chemistry, Debye Institute, Utrecht University, Padualaan 8, 3584 CH Utrecht, The Netherlands
(Received 26 October 2001; published 5 March 2002)

We study isotropic-nematic (*I*-*N*) phase equilibria in the Onsager (-Parsons) model for systems of hard colloidal disks allowing for arbitrary polydispersity in thickness. The phase behavior is investigated by analyzing the exact phase equilibrium equations for Gaussian orientational distribution functions. We observe a strong fractionation effect, with the thicker disks found preferentially in the isotropic phase. Due to this effect, the system may undergo an *I*-*N density inversion* indicating that the mass density of the isotropic phase becomes higher than that of the coexisting nematic phase. This phenomenon has been observed explicitly in experiment. We also encounter a divergence of the *I*-*N* coexistence region for Schulz-distributed parents with polydispersities larger than 46%. An implication of this phenomenon is that the system cannot become fully nematic at high densities but will continue to split off a small fraction of a dilute isotropic phase predominantly containing very thick species.

DOI: 10.1103/PhysRevE.65.031716 PACS number(s): 64.70.Md, 64.60.Cn, 82.70.Dd

I. INTRODUCTION

Since the pioneering work of Zocher and Langmuir [1,2] it has been known that dispersions of highly anisometrical rodlike or platelike colloidal particles exceeding a certain concentration undergo an orientational order-disorder transition from an isotropic state (I), in which the particles are randomly oriented to an orientationally ordered nematic state (N). Onsager [3] first showed that the phase transition can be explained on the basis of purely repulsive interactions between the particles. In his classic work, he explained the phase transition as the result of a competition between orientional entropy that favors the isotropic state and the entropy effect associated with the orientation-dependent excluded volume of the anisometrical particles, which favors the ordered nematic state.

One of the difficulties in quantitatively comparing experimental results with Onsager's predictions is that the colloidal particles are inevitably polydisperse, i.e., they differ in size and shape. The issue of polydispersity and its effect on the interpretation of experimental results has already been addressed by Onsager in his original paper [3]. Later on, extensions of the Onsager treatment allowing for phase diagram calculations for bidisperse and tridisperse systems of rods have led to a rich variety of behavior, such as a widening of the coexistence region, a fractionation effect with the long rods going preferentially into the nematic phase, a reentrant phenomenon, and the possibility of nematic-nematic equilibria [4–7]. However, unlike the case of rodlike particles, the effect of polydispersity on the phase behavior of platelike colloids is only just beginning to be understood.

Recently, a novel model system for polydisperse disks has been developed consisting of sterically stabilized gibbsite platelets [8]. The particles are evidently polydisperse since the platelets strongly differ in both diameter and thickness. The polydispersity for each of the dimensions was estimated at 25%. Quite unexpectedly, the phase behavior of these platelike particles appeared to be more significantly affected by their polydispersity in thickness than by their polydispersity in diameter. While the fractionation in diameter between the isotropic and nematic phases was found to be rather weak [9,10], strong experimental evidence was found for a pronounced thickness fractionation in these systems [9]. The latter effect has led to a surprising phenomenon: the densities of the isotropic and nematic phases may invert upon concentrating a dilute sample in a test tube, indicating that an isotropic *bottom* phase coexists with a nematic *upper* phase [9]. This anomalous behavior, referred to as the *I*-*N* density inversion, can, in principle, be explained by the fractionation in thickness between the phases with the thicker platelets accumulating in the isotropic phase. The fractionation effect, thus, reduces the difference in mass densities between the coexisting phases. Consequently, an inversion occurs when the fractionation effect is strong enough to overrule the difference in thermodynamic number densities of the phases. In a previous study [11], we have verified the possibility of an *I*-*N* inversion in simple binary mixtures of thin and thick hard platelets with common diameter and showed that the inverted state is indeed found in a broad range of plate compositions.

In this paper, we extend our binary model (within the Onsager treatment) to a polydisperse one in which we allow for a *continuous* distribution in thicknesses. As in our previous study, we upgrade Onsager's original second virial approximation quantitatively by applying a renormalization of the second virial term according to Parsons' theory[12]. This approach allows us to incorporate higher virial terms into the free energy, albeit approximately, while requiring only specific knowledge of the two-body excluded volumes. To keep our model analytically tractable, we use the approximate Gaussian trial orientation distribution function (ODF) introduced by Odijk [5], which has a much simpler form than the one originally used by Onsager. Although the Gaussian trial function does not qualify as a thermodynamic equilibrium ODF, it does give reasonable qualitative results for

*FAX: +31-302533870. Email address: G.J.Vroege@chem.uu.nl

highly ordered nematic phases. It is shown that, with the Gaussian ansatz, we may neglect the effect of the thickness on the equilibrium orientations of the platelets implying that the orientations are solely determined by their diameter, which is the same for all species. As a result, the distribution of orientations in the nematic phase can be characterized by a single ODF which holds for all particles. This approach, referred to as the decoupling approximation, allows us to analytically minimize the free energy with respect to the orientational degrees of freedom and leads to an excess free energy obeying a simple moment structure since it only depends on the first two moments of the thickness distribution [13]. Consequently, we are able to obtain the phase behavior exactly by solving the phase equilibrium conditions for polydisperse systems.

In the present paper, we will closely follow the analysis of Clarke *et al.* [14] who recently presented a similar description of the exact phase equilibria in the polydisperse Zwanzig model for hard rods with length polydispersity. An important difference between their polydisperse model and ours is that we are able to retain a system with *continuous* orientations, due to the decoupling approximation. In the Zwanzig model, however, the orientations are discretized as the particle vectors are restricted to lie on one of the Cartesian axes [15].

This paper is structured as follows. In Sec. II A we describe the polydisperse model within the Onsager treatment and derive the free energies for the isotropic and nematic phases. A formulation of the rescaling approach for polydisperse systems is given in Sec. II B. These results are used in Sec. III to study the exact phase equilibrium conditions for this model. In Secs. IV and V we present a detailed analysis of the phase behavior and discuss its most important features. Finally, the conclusions that can be drawn from the present calculations are collected in Sec. VI.

II. MODEL

A. Onsager theory

We consider a system of hard disks with common diameter D but *polydisperse thickness*—such that there is a continuous distribution of lengths L—in a macroscopic volume V. Note that, unlike the opposite case of slender rods, the aspect ratios L/D of the platelets are considered *small* parameters. Within Onsager's approach, the excess free energy describing the (excluded volume) interactions between the particles is truncated after the second virial term. A generalization of the Onsager model to include polydispersity leads to the following expression for the total Helmholtz free energy density f (in units $k_BT \equiv \beta^{-1}$):

$$f \equiv \frac{b\beta F}{V} \sim \int c(l)[\ln c(l) - 1]dl + \int c(l)\omega(l)dl + \int\int c(l)c(l')\rho(l,l')dldl'. \tag{1}$$

Here, $l = L/L_0$ is the relative thickness with respect to some reference length L_0. For the sake of convenience, we have omitted all irrelevant contributions linear in c arising from the standard chemical potentials of the particles. These depend only on the chemical potential of the solvent and the temperature T. The concentrations c are rendered dimensionless by relating them to the orientationally averaged excluded volume per particle between two infinitely thin disks, $b = \pi^2 D^3/16$, via $c(l) = bN(l)/V$ where $N(l)dl$ is the number of particles with relative thickness between l and $l + dl$.

The distribution in thickness $c(l)$ must be normalized according to

$$\int c(l)dl = c_0, \tag{2}$$

where c_0 is the total dimensionless concentration of platelets. The first term in Eq. (1) is exact and represents the ideal free energy of the polydisperse system. The second term is the orientational part involving the parameter ω as a measure for (the negative) of the orientational entropy [3]

$$\omega(l) \equiv \int \psi(l,\theta)\ln[4\pi\psi(l,\theta)]d\Omega, \tag{3}$$

which has its minimum ($\omega \equiv 0$) in the isotropic state but increases as the orientational entropy decreases. The function $\psi(\theta,l)$ is the ODF that describes the distribution of the angles between the normal to the platelet with relative thickness l and the nematic director. The ODF must be normalized according to $\int \psi(\Omega)d\Omega \equiv 1$, where Ω is the solid angle of the platelet's normal vector. In the isotropic state, all orientations are equally probable which implies $\psi_{\rm iso} \equiv 1/4\pi$, independent of l. In the nematic state, however, the platelets are strongly aligned and the ODF will be a sharply peaked distribution.

The last term in Eq. (1) is the excess free energy determined by the interparticle interactions. In the second virial approximation, the interactions between hard particles may be expressed as an excluded-volume entropy depending on the excluded volume between two particles. Onsager gives us the following expression for the excluded volume between two circular disks with relative thicknesses l and l' as a function of their mutual angle γ [3]:

$$v_{\rm excl}(\gamma) = \frac{\pi}{2}D^3\sin\gamma + (l + l')L_0D^2\left\{\frac{\pi}{4} + E(\sin\gamma) + \frac{\pi}{4}|\cos\gamma|\right\} + O(L_0^2D), \tag{4}$$

where $E(k)$ is the complete elliptic integral of the second kind. A measure for the average excluded-volume interaction between platelets of type l and l' is given by the average of its angular dependence

$$\rho(l,l') \equiv (2b)^{-1}\int\int v_{\rm excl}(\gamma)\psi(\theta,l)\psi(\theta',l')d\Omega d\Omega'. \tag{5}$$

The formation of an isotropic state (with ψ constant) or a nematic state [with $\psi(\theta,l)$ a peaked distribution] is caused by a competition between orientational entropy (favoring the isotropic state) and the excluded-volume entropy (favoring the nematic state).

For the isotropic phase, the excluded volume (4) can be readily calculated using the isotropic average $\langle\langle E(\sin\gamma)\rangle\rangle_{\mathrm{iso}} = \pi^2/8$ [3],

$$v_{\mathrm{excl,iso}}(l,l') = \frac{\pi^2}{8}D^3 + (l+l')L_0D^2\left\{\frac{\pi^2}{8}+\frac{3\pi}{8}\right\} + O(L_0^2D). \tag{6}$$

Note that the leading order term (which is equal to $2b$) does not depend on the thickness so that the higher order term must be included to account for the difference in thickness. Substituting Eq. (6) into Eq. (5) yields for the isotropic phase [16],

$$\rho_{\mathrm{iso}}(l,l') = 1 + \frac{L_0}{D}(l+l')\left(1+\frac{3}{\pi}\right) + O(L_0^2/D^2). \tag{7}$$

Note that the second contribution is on the order of L_0/D smaller than the leading order term. Using Eq. (7), together with the isotropic value, $\omega \equiv 0$, we get the following expression for the free energy density in the isotropic phase:

$$f_{\mathrm{iso}} \sim \int c(l)[\ln c(l) - 1]dl + c_0^2 + \left(2+\frac{6}{\pi}\right)\frac{L_0}{D}c_0c_1, \tag{8}$$

where $c_1 \equiv \int c(l) l dl$ is the first moment density of the distribution $c(l)$.

In the nematic phase, matters are more complicated since the ODF is no longer a constant but a sharply peaked function. The excluded-volume entropy is now given by

$$\begin{aligned}\rho_{\mathrm{nem}}(l,l') = {} & \frac{4}{\pi}\int\int |\sin\gamma|\psi(l,\theta)\psi(l',\theta')d\Omega d\Omega' \\ & + \frac{2}{\pi}\frac{L_0}{D}(l+l')\int\int\left[3-\frac{1}{2}\sin^2\gamma + |\cos\gamma|\right] \\ & \times \psi(l,\theta)\psi(l',\theta')d\Omega d\Omega' + O((L_0/D)^2).\end{aligned} \tag{9}$$

Here, the following asymptotic expansion of the elliptic integral has been used [17]:

$$E(\sin\gamma) = \frac{\pi}{2}\left\{1 - \frac{1}{4}\sin^2\gamma + O(\sin^4\gamma)\right\}, \tag{10}$$

which is valid for very small angles γ. This approximation is justified when the ODF is a sharply peaked function. As in Ref. [5], we use Gaussian trial ODFs with variational parameter $\alpha(l)$ to describe the angular distribution of platelets with relative thickness l in the nematic state,

$$\psi(l,\theta) \equiv \begin{cases} \dfrac{\alpha(l)}{4\pi}\exp\left[-\dfrac{1}{2}\alpha(l)\theta^2\right], & 0 \leqslant \theta \leqslant \dfrac{\pi}{2}, \\ \dfrac{\alpha(l)}{4\pi}\exp\left[-\dfrac{1}{2}\alpha(l)(\pi-\theta)^2\right], & \dfrac{\pi}{2} \leqslant \theta \leqslant \pi. \end{cases} \tag{11}$$

Note that α is now a function of l due to the polydispersity. An important advantage of using Gaussian trial ODFs is that ω and ρ are, in principle, analytically tractable. Substituting Eq. (11) in Eq. (3) gives us for the orientational entropy

$$\omega(l) \sim \ln\alpha(l) - 1. \tag{12}$$

For the excluded-volume entropy in the nematic phase we will only retain the leading order terms of its asymptotic expansion for large α

$$\begin{aligned}\rho_{\mathrm{nem}}(l,l') \sim {} & \sqrt{\frac{8}{\pi}[\alpha^{-1}(l)+\alpha^{-1}(l')]} + \frac{8}{\pi}\frac{L_0}{D}(l+l') \\ & \times [1 + O(\alpha^{-1}(l), \alpha^{-1}(l'))].\end{aligned} \tag{13}$$

The leading order L_0/D contribution to ρ_{nem} is simply the excluded volume between two perfectly parallel platelets ($\gamma = 0$) in the nematic phase, $\pi L_0 D^2(l+l')$, divided by the excluded volume $2b$ between two randomly orientated platelets with zero thickness in the isotropic phase. Note that the L_0/D contribution in Eq. (13) remains constant up to order $O(\alpha^{-1})$.

The next step is to insert Eqs. (12) and (13) into Eq. (1) and minimize the free energy density with respect to the orientational degrees of freedom via a functional differentiation that leads to the stationarity condition $\delta f/\delta\alpha(l) \equiv 0$. Retaining the $O(\alpha^{-1}(l))$ in Eq. (13) would then give a nonlinear integral equation to be solved along with the phase equilibrium conditions (see paragraph below) which is a very complicated task. In our approach, we choose to neglect the $O(\alpha^{-1})$ term in Eq. (13), whose contribution is on the order of $(D/L_0)\alpha^{1/2}$ smaller than the leading term in the asymptotic expansion of ρ_{nem}. Since α is usually very large for the nematic phase, this approximation can be readily justified. An essential implication of the approach is that the second term in Eq. (13), which is the only part depending on the thickness l, vanishes upon minimizing the free energy. Since there is no contribution depending explicitly on l we may simply substitute $\alpha(l) = \alpha(l') = \alpha$ in Eqs. (12) and (13) to obtain after minimization,

$$\alpha(l) = \alpha = \frac{4c_0^2}{\pi} \quad \text{for all } l, \tag{14}$$

which is the same result as for a monodisperse system [18]. A formal derivation of this result is given in the Appendix. The physical interpretation of the approximation is that the orientations of the platelets are solely determined by the diameter—which is identical for all particles—and not by their thickness. Consequently, the orientational degrees of freedom are *decoupled* from the degrees of freedom that determine the shape of the thickness distribution.

Using Eq. (14) and substituting the expressions for ω and ρ back into the free energy (1) then yields the following simple expression for the free energy in the nematic phase:

$$f_{\mathrm{nem}} \sim \left(\ln\frac{4}{\pi} + 1 \right) c_0 + \int c(l)[\ln c(l) - 1]dl + 2c_0 \ln c_0 + \frac{16}{\pi}\frac{L_0}{D} c_0 c_1 . \tag{15}$$

The results given thus far apply to the second virial approximation, meaning that higher order correlations between the disks are neglected. However, Onsager already pointed out in his original paper that a truncation of the free energy after the second virial term is an approach that, although valid for sufficiently elongated needles (with aspect ratios exceeding 100), cannot be justified quantitatively for disklike particles. The reason for this is that disks always have a nonzero probability of intersection and thus a finite excluded volume even at zero thickness ($L_0/D=0$). The relative importance of three-body interactions in terms of the ratio B_3/B_2^2 (with B_3 the third virial coefficient) has been estimated by Onsager at $O(1)$ [3]. More accurate predictions were obtained from computer simulations [21], giving $B_3/B_2^2 \approx 0.51$ for disks with aspect ratio $L/D=0.1$. These results clearly indicate that many-body interactions will undoubtedly play a role in systems of disks, even at low concentrations. Therefore, in order to make credible comparisons with the experimental results, we have to somehow account for the effect of higher virial terms. The most straightforward way to improve the Onsager theory would be to include higher virial terms directly. Although this is, in principle, feasible, it turns out to be a very complicated method [19,20]. A much easier way to upgrade the original theory is by indirect inclusion of many-body terms using the Carnahan-Starling excess free energy for hard spheres. This approach, which was originally formulated by Parsons [12], will be discussed next.

B. Parsons' approach

In Parsons' approach, the Carnahan-Starling expression for hard spheres is applied to the system of anisometrical particles under consideration, using the orientationally averaged second virial coefficient as a scaling factor. The justification for the approach lies in a decoupling approximation such that the orientational and translational degrees of freedom for a system of anisometrical particles may be treated separately [12]. An important implication of Parsons' theory is that it incorporates many-body effects (albeit in an average way) while requiring only explicit knowledge of the two-particles interactions as embodied in the second virial term of the free energy. For this reason, the approach is much easier to use than the straightforward option of direct inclusion of higher virial terms [19,20].

The quantitative success of the approach has initially been confirmed by Lee [22,23], at least for hard rodlike particles. He calculated the *I-N* transition densities for a system of hard ellipsoidal particles with aspect ratio $L/D=5$ and found results that were in close agreement with computer simulations. More extensive comparisons between the Onsager-Parsons theory and computer simulations were made by McGrother *et al.* [24] for short hard spherocylinders ($L/D<5$) and by Camp *et al.* [25] for hard prolate ellipsoids ($5 \leqslant L/D \leqslant 20$). In both cases, the transition densities as found from the theory agreed very well with the simulation results. In a similar study, Camp and co-workers [26,27] showed that Parsons' approach also worked well for mixtures of rodlike and platelike ellipsoids, showing improved quantitative agreement with computer simulations over the Onsager theory and the *y*-expansion approach. The latter method, which is due to Barboy and Gelbart [28], provides direct inclusion of higher virial terms by a recasting of the free energy in terms of a new density variable *y*. However, unlike the case of hard rods, no systematic comparative study has been reported so far on the effect of Parsons rescaling on the *I-N* transition in systems of hard platelike particles (i.e., oblate ellipsoids or cylindrical disks).

As already mentioned, the starting point of the approach is the semiempirical Carnahan-Starling excess free energy for hard spheres [29],

$$f_{\mathrm{CS}}(\phi) = \frac{\beta F_{\mathrm{CS}}^{\mathrm{ex}}}{N} = \frac{\phi(4-3\phi)}{(1-\phi)^2}, \tag{16}$$

where ϕ is the volume fraction of hard spheres. For a one-component system of hard anisometrical particles this free energy is multiplied by the prefactor $\langle\langle v_{\mathrm{excl}}\rangle\rangle/8v_0$ with v_0 the particle volume and $\langle\langle v_{\mathrm{excl}}\rangle\rangle$ the average excluded volume. Note that $\langle\langle v_{\mathrm{excl}}\rangle\rangle/8v_0=1$, in the case of hard spheres. For a monodisperse system of platelets the Parsons excess free energy density (denoted by "P") can be written as

$$\frac{b\beta F_{\mathrm{P}}^{\mathrm{ex}}}{V} = \frac{(4-3\phi)}{4(1-\phi)^2} c_0^2 \rho \tag{17}$$

where ρ is given by Eq. (5) for the monodisperse case (i.e., $l=l'=1$). We may generalize the above expression for a polydisperse system in the following way:

$$\frac{b\beta F_{\mathrm{P}}^{\mathrm{ex}}}{V} = \frac{(4-3\phi)}{4(1-\phi)^2} \int\int c(l)c(l')\rho(l,l')dldl' = \frac{f_{\mathrm{CS}}(\phi)}{4\phi}\frac{b\beta F_{\mathrm{O}}^{\mathrm{ex}}}{V}, \tag{18}$$

where $b\beta F_{\mathrm{O}}^{\mathrm{ex}}/V$ is the excess free energy density in the Onsager model, given by the last term in Eq. (1). Furthermore, ϕ is the total volume fraction of platelets, related to the thickness distribution $c(l)$ via

$$\phi = \frac{4}{\pi}\frac{L_0}{D}\int c(l)ldl = \frac{4}{\pi}\frac{L_0}{D}c_1 . \tag{19}$$

From Eq. (18) we see that Parsons' approach essentially comprises a rescaling of the excess free energy using the Carnahan-Starling result for hard spheres. Replacing the last term in Eq. (1) by Eq. (18) gives us the Onsager-Parsons free energy for a polydisperse system of hard platelets. For the isotropic phase we thus obtain

$$f^{\mathrm{P}}_{\mathrm{iso}} \sim \int c(l)[\ln c(l) - 1]dl + \frac{f_{\mathrm{CS}}(\phi)}{4\phi}\left[c_0^2 + \left(2 + \frac{6}{\pi}\right)\frac{L_0}{D}c_0 c_1\right]. \quad (20)$$

For the nematic phase, matters are slightly more complicated because of the minimization step. Minimizing with respect to α now yields

$$\alpha \sim \frac{4}{\pi}c_0^2\left(\frac{f_{\mathrm{CS}}(\phi)}{4\phi}\right)^2 \quad (21)$$

and the Onsager-Parsons free energy for the nematic phase reads

$$f^{\mathrm{P}}_{\mathrm{nem}} \sim \left(\ln\frac{4}{\pi} + 1\right)c_0 + \int c(l)[\ln c(l) - 1]dl + 2c_0 \ln\left[c_0 \frac{f_{\mathrm{CS}}(\phi)}{4\phi}\right] + \frac{f_{\mathrm{CS}}(\phi)}{4\phi}\frac{16}{\pi}\frac{L_0}{D}c_0 c_1. \quad (22)$$

III. COEXISTENCE CONDITIONS

To derive the conditions for phase equilibria in the polydisperse model, we must know the expressions for the chemical potential $\mu(l)$—which, due to the polydispersity, is a function of the relative thickness l—and the osmotic pressure Π. The chemical potential can be derived by functional differentiation of the free energy with respect to the thickness distribution $c(l)$,

$$\beta\mu(l) = \frac{\delta f}{\delta c(l)}. \quad (23)$$

Using Eqs. (8) and (15) we obtain for the Onsager model,

$$\beta\mu_{\mathrm{iso}}(l) = \ln c(l) + 2c_0 + \left(2 + \frac{6}{\pi}\right)\frac{L_0}{D}(c_0 l + c_1),$$

$$\beta\mu_{\mathrm{nem}}(l) = \ln c(l) + 2\ln c_0 + \frac{16}{\pi}\frac{L_0}{D}(c_0 l + c_1) + \left(\ln\frac{4}{\pi} + 3\right). \quad (24)$$

The osmotic pressure can be written in terms of the chemical potential and the free energy via

$$b\beta\Pi \equiv -f + \beta\int dl\, c(l)\mu(l), \quad (25)$$

which yields

$$b\beta\Pi_{\mathrm{iso}} \sim c_0 + c_0^2 + \left(2 + \frac{6}{\pi}\right)\frac{L_0}{D}c_0 c_1,$$

$$b\beta\Pi_{\mathrm{nem}} \sim 3c_0 + \frac{16}{\pi}\frac{L_0}{D}c_0 c_1. \quad (26)$$

Similar expressions for the chemical potentials and osmotic pressures can be derived straightforwardly from the Onsager-Parsons free energy using Eqs. (20) and (22). These expression are, however, more elaborate due to the presence of $f_{CS}(\phi)$ and its derivatives.

We can now state the conditions for the coexistence between the isotropic and nematic daughter phases into which a parent phase with thickness distribution $c^{(0)}(l)$ is assumed to have split. From Eq. (24), equality of chemical potentials of both phases is obeyed exactly if the distributions in the phases have the following form:

$$c^{(a)}(l) = W(l)\exp[\xi^{(a)}(l)], \quad a = I,N, \quad (27)$$

where $W(l) \equiv \exp[\beta\mu(l)]$ must be a function common to both phases, since $\mu_{\mathrm{iso}}(l) = \mu_{\mathrm{nem}}(l) = \mu(l)$. For the nonrescaled Onsager free energy the functions $\xi(l)$ are given by

$$\xi^{(I)}(l) = -\left(2 + \frac{6}{\pi}\right)\frac{L_0}{D}(c_0^{(I)} l + c_1^{(I)}) - 2c_0^{(I)},$$

$$\xi^{(N)}(l) = -\frac{16}{\pi}\frac{L_0}{D}(c_0^{(N)} l + c_1^{(N)}) - 2c_0^{(N)}\ln c_0^{(N)} - \left(\ln\frac{4}{\pi} + 3\right). \quad (28)$$

Again, we can obtain similar expressions from the rescaled Onsager-Parsons free energy. Furthermore, conservation of matter requires

$$c^{(0)}(l) = \gamma c^{(I)}(l) + (1-\gamma)c^{(N)}(l), \quad (29)$$

where γ denotes the fraction of the system volume occupied by the isotropic phase. Using Eq. (29), we can express $W(l)$ in terms of the parent distribution $c^{(0)}(l)$,

$$c^{(a)}(l) = c^{(0)}(l)\frac{\exp[\xi^{(a)}(l)]}{\gamma\exp[\xi^{(I)}(l)] + (1-\gamma)\exp[\xi^{(N)}(l)]}, \quad a = I,N. \quad (30)$$

The moment densities (c_0 and c_1), which determine the osmotic pressures (26) and the functions $\xi^{(a)}(l)$ are obtained by integrations over these distributions

$$c_0^{(a)} = \int c^{(a)}(l)dl \quad \text{and} \quad c_1^{(a)} = \int l c^{(a)}(l)dl, \quad a = I,N. \quad (31)$$

In order to solve the self-consistency equations above we must specify a parent distribution $c^{(0)}(l)$. In the present study we assume that the thicknesses are distributed along a Schulz distribution

$$c^{(0)}(l) = c_0^{(0)}\frac{(1+z)^{1+z}}{\Gamma(1+z)}l^z\exp[-(z+1)l], \quad (32)$$

which is normalized according to $\int c^{(0)}(l)dl = c_0^{(0)}$, with $c_0^{(0)}$ the overall particle concentration in the parent phase and has an average thickness $m_1^{(0)} \equiv c_1^{(0)}/c_0^{(0)} = 1$. The latter implies that we may identify the ratio L_0/D involving the reference

length as the mean aspect ratio of the platelets. The polydispersity (defined as the relative standard deviation σ) is related to the parameter z via

$$\sigma \equiv \left([m_1]^{-2} \int l^2 \frac{c^{(0)}(l)}{c_0} dl - 1 \right)^{1/2} = (1+z)^{-1/2}. \quad (33)$$

We are now ready to investigate the coexistence between the isotropic and nematic phase in our polydisperse model. Before discussing the full coexistence problem, we will first attempt to derive simple expressions for the so-called cloud point and shadow curves that locate the onset of phase separation. At the cloud point, the parent phase coexists with an infinitesimal amount of a new phase, called the ''shadow'' phase. Accordingly, at the isotropic cloud point only an infinitesimal amount of nematic phase (''shadow phase'') has emerged and so the distribution of the isotropic phase is only negligibly perturbed away from the parent. Hence, for the isotropic cloud point we set $\gamma=1$ in Eq. (30) so that

$$c^{(I)}(l) = c^{(0)}(l),$$

$$c^{(N)}(l) = c^{(0)}(l) \exp[\xi^{(N)}(l) - \xi^{(I)}(l)]. \quad (34)$$

Substituting this into Eq. (31) gives $c_0^{(I)} = c_1^{(I)} = c_0^{(0)}$, which implies that the isotropic phase is identified as the parent. The moment densities for the associated nematic shadow are then given by

$$c_0^{(N)} = c_0^{(0)} \frac{(1+z)^{1+z}}{\Gamma(1+z)} \exp[\Delta\xi''] \times \int l^z \exp\{[\Delta\xi' - (z+1)]l\} dl,$$

$$c_1^{(N)} = c_0^{(0)} \frac{(1+z)^{1+z}}{\Gamma(1+z)} \exp[\Delta\xi''] \times \int l^{z+1} \exp\{[\Delta\xi' - (z+1)]l\} dl, \quad (35)$$

where we have rewritten $\xi^{(N)}(l) - \xi^{(I)}(l)$ by splitting it into parts, according to

$$\xi^{(N)}(l) - \xi^{(I)}(l) \equiv \Delta\xi' l + \Delta\xi''. \quad (36)$$

Note that $\Delta\xi'$ and $\Delta\xi''$ are both independent of l. The integrals can be worked out straightforwardly to obtain the following coupled set of consistency equations:

$$c_0^{(N)} = c_0^{(0)} \exp[\Delta\xi''] \left(\frac{z+1}{(z+1) - \Delta\xi'} \right)^{z+1},$$

$$c_1^{(N)} = c_0^{(0)} \exp[\Delta\xi''] \left(\frac{z+1}{(z+1) - \Delta\xi'} \right)^{z+2}. \quad (37)$$

The same analysis can be done for the nematic cloud point and shadow curves by setting $\gamma=0$ so that the nematic phase is identified as the parent phase, thus $c_0^{(N)} = c_1^{(N)} = c_0^{(0)}$. The densities of the shadow phase ($c_0^{(I)}$ and $c_1^{(I)}$) are given by similar equations as Eq. (37). To track down the cloud point and shadow curves we must solve the coupled set of consistency equations under the condition of equal osmotic pressures $\Pi_{\rm iso} = \Pi_{\rm nem}$.

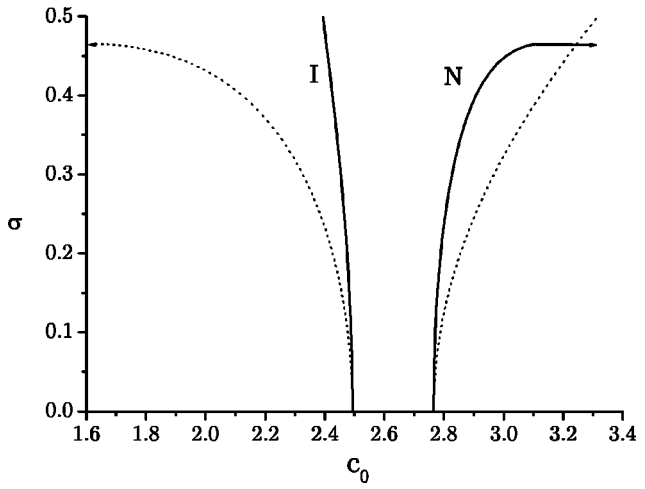

FIG. 1. The isotropic (I) and nematic (N) cloud point curves (solid) and the corresponding shadow curves (dotted) showing the concentrations of the coexisting phases c_0 as a function of the parent polydispersity σ. At $\sigma=0$, the isotropic cloud point meets the shadow of the nematic cloud point and vice versa, as it should.

In the coexistence region, which is bounded by the isotropic and nematic cloud points, both phases coexist in finite amounts, implying $0<\gamma<1$. From an experimental standpoint, the results must be restricted to lie on a physical dilution line along which the shape of the parent distribution, $c^{(0)}(l)/c_0^{(0)}$, is kept fixed while the overall parent concentration $c_0^{(0)}$ is subject to variation. To calculate the evolution of the densities inside the coexistence region we have to solve the four integral equations (31) along with the equation of osmotic pressure. For a given polydispersity of the parent, there appear six variables in these equations (i.e., the five density variables $c_0^{(I)}, c_1^{(I)}, c_0^{(N)}, c_1^{(N)}, c_0^{(0)}$ plus γ) implying that one variable can be freely chosen. Numerically, rather than changing the overall parent density $c_0^{(0)}$, it has proven to be more convenient to construct a scheme in which γ is varied between 0 and 1 and the corresponding densities are calculated self-consistently [14].

IV. RESULTS

A. Cloud point and shadow curves

The results for the cloud point and shadow curves are shown in Figs. 1–3. These curves are calculated from the rescaled Onsager-Parsons free energy, Eqs. (20) and (22). In all calculations we used a mean aspect ratio L_0/D of 0.13, which value is in close agreement with the average aspect-ratio of the gibbsite platelets used in experiment [9]. From Fig. 1 we see that the coexistence region broadens significantly as the polydispersity of the parent becomes higher, in particular, at $\sigma>0.4$. A notable feature is the divergence of the two-phase region at $\sigma>0.46$ indicating that the concen-

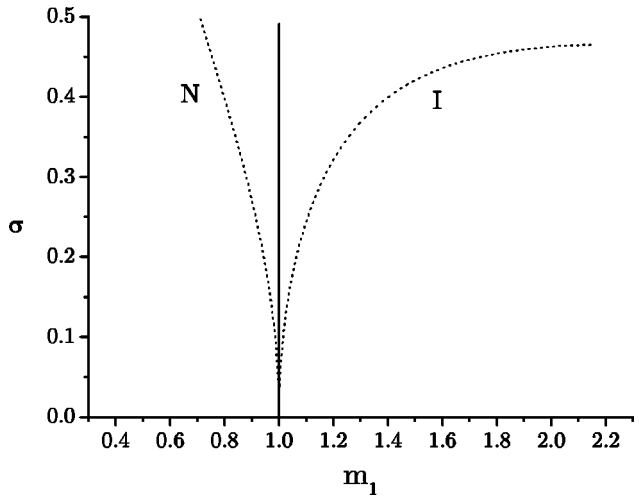

FIG. 2. The average platelet thickness m_1 in the isotropic and nematic shadow phases as a function of the parent polydispersity σ. Note that both cloud point curves are identical to the parent and, therefore, have $m_1 = m_1^{(0)} = 1$.

tration of the nematic cloud shifts to infinity while the concentration of the corresponding shadow rapidly moves to zero. This divergent behavior is not observed for the isotropic cloud point and shadow. Although the concentration of the isotropic shadow increases rapidly with increasing polydispersity, it remains finite even at $\sigma \gg 0.5$. In Fig. 2 we show the average thickness of the platelets in the isotropic and nematic phases. A strong fractionation effect is observed, with the thicker platelets going preferentially into the isotropic phase. At high polydispersities (>0.4) the effect becomes very pronounced since the average thickness in the isotropic phase may rise up to twice that in the nematic phase. Again we observe a divergence in the nematic shadow at $\sigma > 0.46$ indicating that the average thickness of platelets in the isotropic phase rapidly shifts to infinity.

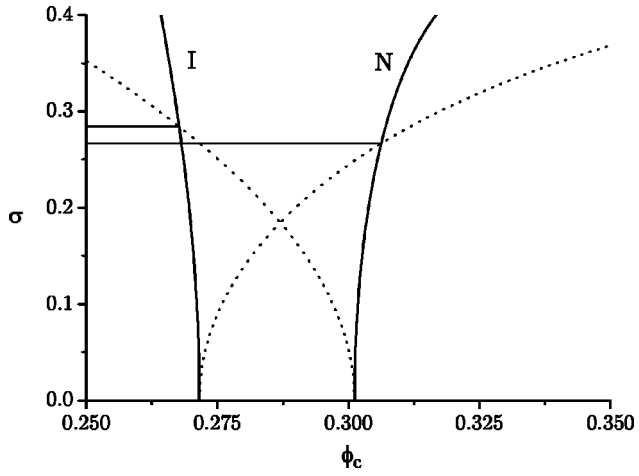

FIG. 3. The isotropic (I) and nematic (N) cloud point curves (solid) and the corresponding shadow curves (dotted) in terms of the core volume fractions ϕ_c of the coexisting phases as a function of the parent polydispersity σ. Recall that ϕ_c is linearly proportional to the mass density of the phase. The horizontal lines denote the points where the cloud and shadow phases have equal mass densities. For polydispersities above the "threshold" value $\sigma = 0.267$ (indicated by the lower horizontal line) an inverted state will be found at which the isotropic phase is denser than the nematic phase. In the small interval between the two horizontal lines ($0.267 < \sigma < 0.284$) a density inversion takes place inside the coexistence region.

In this paper, we also investigate the possibility of an *I-N* density inversion, as observed in experiment. A density inversion implies that, at some point in the two-phase region, the mass density of isotropic becomes higher than that of the nematic phase so that the coexisting phases may turn upside down in a test tube. To verify this, we have to calculate the mass density of the phases. In Ref. [11], rather than calculating the mass density itself, we defined the core volume fraction ϕ_{core} of the platelets as a more convenient density variable. It is easy to show that ϕ_{core} is linearly proportional to the mass density of the gibbsite platelets used in experiment [9]. The core volume fraction can be calculated from

$$\phi_{\text{core}} = \frac{\pi}{4}\frac{N}{V}D^2 \int c(l)(L - 2\delta)dl \tag{38}$$

$$= \frac{4}{\pi}\frac{L_0}{D}c_1 - \frac{8}{\pi}c_0\frac{\delta}{D}, \tag{39}$$

where δ/D is the thickness of the stabilizing polymer layer grafted onto the gibbsite platelets relative to the average diameter of the platelets. From the experimental results [9] we estimate $\delta/D = 4/180$. The resulting plot is shown in Fig. 3. We indeed observe an inverted state (i.e., the isotropic phase being more dense than the nematic phase) at polydispersities roughly above 30%. This implies that, at these polydispersities, the fractionation effect is strong enough to overcome the difference in number densities between the coexisting phases. In particular, we can identify a small interval $0.267 < \sigma < 0.284$ where an *I-N density inversion* takes places inside the two-phase region, in accordance with the experimental observations [30]. In these cases, the normal state will be found at the beginning of the coexistence region (close to the isotropic cloud point) but an inverted state will be found close to the nematic cloud point. Clearly, there must be a point $0 < \gamma < 1$ somewhere in the two-phase region where a density inversion takes place. To find this point, we have to resort to the full coexistence problem.

B. Inside the coexistence region

In Fig. 4 we show the evolution of the densities and average thicknesses across the coexistence region for a fixed polydispersity of the parent phase. As expected, both the densities and the averages m_1 vary smoothly between the isotropic and nematic cloud points that delimit the two-phase coexistence region. We see that the average thickness is always higher in the isotropic phase than in the nematic phase, as we expect from Fig. 2. A more detailed picture of the fractionation effect can be seen in Fig. 5 where we have depicted the thickness distributions in the coexisting phases.

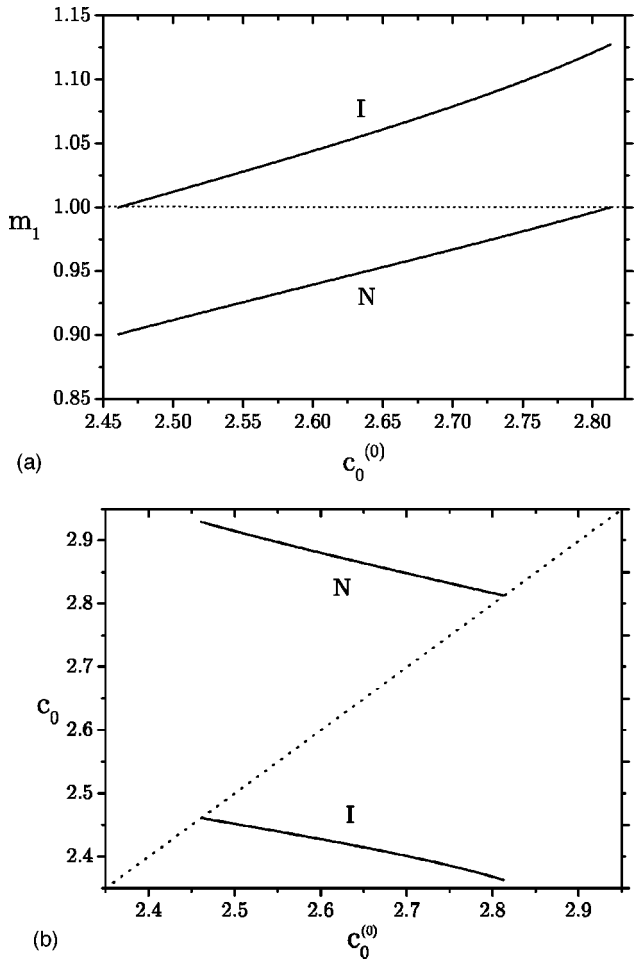

FIG. 4. (a) The average thickness m_1 in the coexisting phases as a function of the concentration of the parent phase $c_0^{(0)}$ for a polydispersity $\sigma=0.27$. The isotropic and nematic cloud points, which delimit the coexistence region, are located at the points where the curves meet the dilution line ($m_1^{(0)}=1$, dotted line). (b) Evolution of the concentrations of the coexisting phases across the two-phase region for the same polydispersity. The dotted line represents the dilution line ($c_0=c_0^{(0)}$).

In Fig. 6 we have plotted the variation of the core volume fractions for a parent with $\sigma=0.27$ as the coexistence region is crossed. According to Fig. 3, this parent should undergo a density inversion somewhere inside the coexistence region. Figure 6 shows that there is indeed an inversion, albeit very close to the nematic cloud point in this case. The inversion occurs at a parent volume fraction $\phi=0.461$ which corresponds to $\gamma=0.073$. So the inversion takes place when the volume occupied by the isotropic phase has decreased to about 7% of the total system volume. Finally, in Fig. 7, we show the polydispersities of the daughter phases inside the coexistence region for the same parent as in Fig. 6. At coexistence, both daughter phases have a lower polydispersity than the parent phase due to the fractionation effect. However, the deviations are very small ($\Delta\sigma<0.006$) for this particular parent polydispersity. Note that the polydispersities of the daughter phases reach their minimum around $\gamma=0.5$, i.e., when the isotropic and nematic phases coexist in approximately equal amounts.

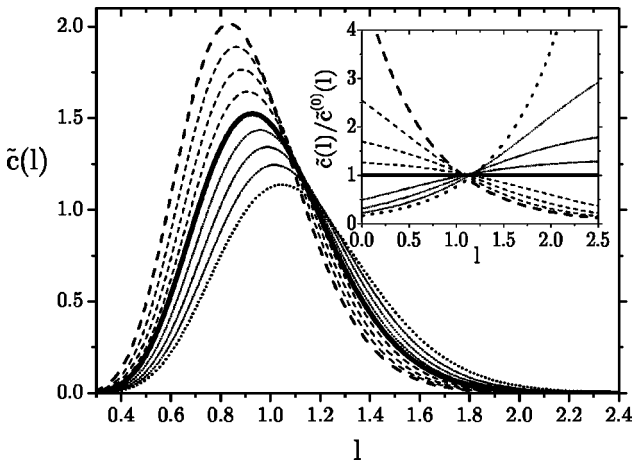

FIG. 5. The normalized thickness distribution $\tilde{c}(l)\equiv c(l)/c_0^{(0)}$ in the isotropic and nematic phases at polydispersity $\sigma=0.27$ for various γ. Bold dashed curve: distribution in the nematic shadow at the isotropic cloud point ($\gamma=1$). Bold dotted curve: distribution in the isotropic shadow at the nematic cloud point ($\gamma=0$). The distributions in the isotropic and nematic phases at these points are given by the parent (bold solid curve). The intermediate curves represent, from top to bottom, the distributions of the coexisting isotropic (dotted) and nematic (dashed) phases for $\gamma=0.75$, 0.5 and $\gamma=0.25$, respectively. The inset shows the ratio of the thickness distributions to that of the parent.

V. DISCUSSION

We have studied *I-N* phase equilibria in the Onsager-Parsons model for hard disks allowing for polydispersity in thickness. We have analyzed the onset of phase separation by calculating the cloud point and shadow curves—which delimit the two-phase coexistence region—as a function of the polydispersity of the parent. A significant broadening of the coexistence region is observed for moderately high polydis-

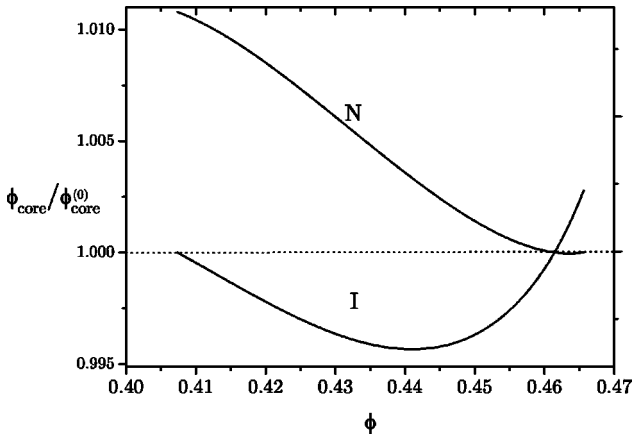

FIG. 6. The ratio of the core volume fraction of the isotropic and nematic phases relative to the parental one for $\sigma=0.27$ plotted vs the volume fraction of platelets ϕ in the parent phase. The dotted line represents the dilution line ($\phi_{\rm core}/\phi_{\rm core}^{(0)}=1$). The intersection point indicates that a density inversion will occur at volume fractions $\phi>0.461$. In these cases, the isotropic phase will be denser than the nematic phase.

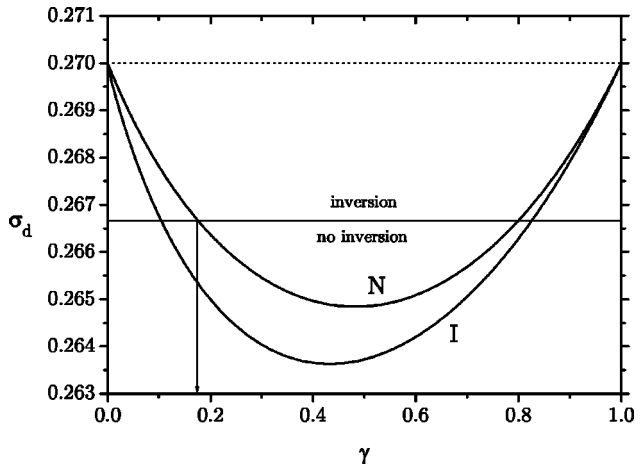

FIG. 7. Evolution of the polydispersities σ_d of the coexisting isotropic and nematic daughter phases across the coexistence region for a parent with $\sigma=0.27$ plotted vs the fraction γ of the system volume occupied by the isotropic phase. The solid horizontal line indicates the ''threshold'' polydispersity $\sigma=0.267$ (see also Fig. 3). A parent phase with a polydispersity below this value will not exhibit a density inversion during phase separation.

persities ($\sigma<0.3$). We also see a strong fractionation effect with the thick species preferentially occupying the isotropic phase. Although the biphasic widening and fractionation effect are generic properties observed in many polydisperse systems [18,31], it is rather surprising that these effects occur so strongly in mixtures of disks which only differ in thickness. Recall from Eq. (6), that the thickness only marginally contributes to the excluded volume provided that the aspect ratios L_0/D are small parameters. Hence, one might have anticipated that the effect of thickness on the phase behavior of disks is unlikely to be significant.

Even more striking is the infinite broadening of the coexistence region at polydispersities $\sigma>0.46$ due to a divergence of the nematic cloud point and shadow curves (see Figs. 1 and 2). This phenomenon can be interpreted as follows. When a dilute parent phase with $\sigma>0.46$ is concentrated it starts to phase separate at the isotropic cloud point, initially splitting off an infinitesimal amount of nematic phase (the shadow). The fraction of nematic phase increases upon further concentrating the parent sample. However, as we see from Fig. 1, the parent will never reach the associated nematic cloud point. Regardless of the concentration of the parent phase, the system always splits off a tiny fraction of an (increasingly dilute) isotropic phase which, according to Fig. 2, will accommodate increasingly thicker platelets. This means that the system never becomes fully nematic, irrespective of the concentration of the parent. The question now arises whether this is a realistic picture. It may be possible that the anomalous behavior stems from the fact that the thickness distribution adopted here is unbounded, meaning that there is a nonzero probability of finding species with very large (potentially infinite) thicknesses for which the aspect ratio is no longer a small parameter. Therefore, different results might be obtained when considering a truncation of the distribution at a certain limit value $l_{\rm lim}$ (say $l_{\rm lim}=3$), so that $c(l)\equiv 0$ for $l>l_{\rm lim}$. Adopting a truncated distribution like this is probably more realistic from an experimental point of view.

In a previous paper [11] we made a theoretical investigation of the experimentally observed *I*-*N* density inversion by considering a simple binary mixture of platelets with differing thickness. Although the density inversion could readily be accounted for within this model, we were not able to explain another peculiar observation encountered in the experimental work [9]. As part of their experimental survey, Van der Kooij *et al.* performed an additional fractionation experiment in which a suspension was brought to a volume fraction ($\phi=0.29$) close to the nematic cloud point ($\phi=0.30$) and left to phase separate. The nematic upper phase was separated from the isotropic bottom phase and subsequently diluted. A remarkable observation was that this system did not exhibit a density inversion at any point in the isotropic-nematic coexistence region. This striking observation could however not be explained, for fundamental reasons, on the basis of the binary model for these systems, as discussed in Ref. [11].

In the present study we have extended our binary model to a polydisperse one, meaning that we allow for a continuous distribution in thickness instead of just two different species. We may now consider the polydispersities of the coexisting isotropic and nematic daughter phases for a given parent distribution. In Fig. 7 these results are plotted for a parent with $\sigma=0.27$. As noted in the previous paragraph, the daughter phases have $\sigma<0.27$, which is a direct consequence of the fractionation in thickness during phase separation. In this figure we also indicated the ''threshold'' polydispersity (see Fig. 3) below which the fractionation effect is too weak to accomplish an inversion of densities. So any daughter phase with a polydispersity below the threshold will probably not show an *I*-*N* density inversion if this phase were to be isolated and subsequently diluted or concentrated (as the new parent phase). Despite the fact that the distributions in the daughter phases no longer exactly obey the Schulz form, the deviations will generally be very small close to the isotropic and nematic cloud points. Since the polydispersity of the parent may be chosen arbitrarily, we can make a reasonable account for the experimental observations by picking a parent polydispersity which is just above the ''threshold'' as indicated in Fig. 7. In that case, the polydispersities of the daughter phases will cross the threshold close to the nematic cloud point (i.e., when the system is almost fully nematic). Subsequent isolation and dilution of the near-Schulz nematic parent would then give a phase separation into an isotropic phase that is less dense than the nematic phase and hence the density inversion has disappeared.

An issue that is not addressed in this paper is the possibility of a demixing transition in the nematic phase. For binary mixtures of thin and thick platelets a stable demixing transition of the nematic phase could readily be established [11]. It was shown that the transition occurs for any thickness ratio provided that the osmotic pressure is sufficiently high. Recently, Cuesta [32] showed that, for a polydisperse hard sphere fluid distributed along a (single-peaked) log-normal distribution, a fluid-fluid demixing transition might occur at polydispersities larger than 160%. However, only the spin-

odal instability was analyzed there without considering the coexistence conditions for the fluid phases. The possibility of a scenario similar to the one found by Cuesta for a polydisperse system of platelets distributed along a single-peaked thickness distribution is an intriguing issue. Although investigation is going on, there are no conclusive results so far on this matter [33].

VI. CONCLUSIONS

We have investigated the effect of thickness polydispersity on the isotropic-nematic phase equilibria in the Onsager-Parsons model for hard disks. We show that it is justified, at least within the Gaussian approximation, to decouple the orientational degrees of freedom from the degrees of freedom which determine the thickness distribution. This approach, which implies that the orientations of the platelets are solely determined by the diameter of the platelets and *not* by the thickness, allows us to perform the free energy minimization with respect the orientations analytically and analyze the exact phase equilibrium conditions. In this way, rather than having to discretize the orientations such as in the Zwanzig model [14], we retain a system with *continuous* orientational degrees of freedom. Apart from more generally observed features such as a widening of the biphasic gap and a fractionation effect, with the thicker species accumulating in the isotropic phase, we observe a divergence of the coexistence region at $\sigma > 0.46$ indicating that the system never becomes fully nematic at high densities but will always split off a small fraction of a dilute isotropic phase predominantly containing very thick species.

In addition, we observe an *I-N* density inversion inside the coexistence region at $0.267 < \sigma < 0.284$, which is in qualitative agreement with the experimental observations. A practical implication of the inversion is that upon concentrating a dilute parent phase with polydispersity around 27% in a test tube an isotropic upper phase will be formed initially (near the isotropic cloud point) whereas an isotropic bottom phase will be found close to the nematic phase boundary (see Fig. 3) [30]. This phenomenon has been observed experimentally in systems of polydisperse colloidal gibbsite platelets [9]. Within our polydisperse model, we also account for a particular dilution experiment performed in Ref. [9]. These observations could not be explained on the basis of a binary model for these systems developed by us in a previous study [11].

ACKNOWLEDGMENT

We gratefully acknowledge Henk Lekkerkerker for stimulating discussions.

APPENDIX

Inserting Eqs. (12) and (13) into the free energy (1) and performing a functional differentiation with respect to $\alpha(l)$ yields

$$\frac{\delta f}{\delta \alpha(l)} \sim \frac{c(l)}{\alpha(l)} - \sqrt{\frac{8}{\pi}} \frac{c(l)}{\alpha^2(l)} \int c(l') \left(\frac{1}{\alpha(l)} + \frac{1}{\alpha(l')} \right)^{-1/2} dl'. \tag{A1}$$

Applying the stationarity condition $\delta f / \delta \alpha(l) = 0$ gives after some rearrangements

$$\alpha^{1/2}(l) \sim \sqrt{\frac{8}{\pi}} \int \frac{c(l')}{[1+\alpha(l)/\alpha(l')]^{1/2}} dl'. \tag{A2}$$

Obviously, a similar expression is obtained for $\alpha(l')$. It is convenient to combine both expressions using the ratio $Q(l,l') \equiv \alpha(l)/\alpha(l')$ to obtain

$$Q^{1/2}(l,l') \sim \int \frac{\tilde{c}(l'')}{[1+Q(l,l'')]^{1/2}} dl'' \Big/ \int \frac{\tilde{c}(l''')}{[1+Q(l',l''')]^{1/2}} \times dl''', \tag{A3}$$

which is an implicit equation for $Q(l,l')$. Note that Q only depends on the normalized distributions $\tilde{c}(l) \equiv c(l)/c_0$ and not on the overall concentration c_0 of the nematic phase. One readily concludes that $Q(l,l') = Q(1,1) = 1$ is a trivial solution of Eq. (A3). Using this in Eq. (A2) thus yields the following solution for the stationarity condition within the decoupling approximation

$$\alpha \sim \left(\sqrt{\frac{8}{\pi}} \int \frac{c(l')}{2^{1/2}} dl' \right)^2,$$

$$\alpha \sim \frac{4c_0^2}{\pi}, \tag{A4}$$

independent of the thickness l.

[1] H. Zocher, Z. Anorg. Allg. Chem. **147**, 91 (1925).
[2] I. Langmuir, J. Chem. Phys. **6**, 873 (1938).
[3] L. Onsager, Ann. N.Y. Acad. Sci. **51**, 627 (1949).
[4] H. N. W. Lekkerkerker, P. Coulon, R. van der Hagen, and R. Deblieck, J. Chem. Phys. **80**, 3427 (1984).
[5] T. Odijk and H. N. W. Lekkerkerker, J. Phys. Chem. **89**, 2090 (1985).
[6] T. M. Birshtein, B. I. Kolegov, and V. A. Pryamitsin, Polym. Sci. U.S.S.R. **30**, 316 (1988).
[7] G. J. Vroege and H. N. W. Lekkerkerker, J. Phys. Chem. **97**, 3601 (1993).
[8] F. M. van der Kooij and H. N. W. Lekkerkerker, J. Phys. Chem. B **102**, 7829 (1998).
[9] F. M. van der Kooij, D. van der Beek, and H. N. W. Lekkerkerker, J. Phys. Chem. B **105**, 1696 (2001).
[10] M. A. Bates and D. Frenkel, J. Chem. Phys. **110**, 6553 (1999).
[11] H. H. Wensink, G. J. Vroege, and H. N. W. Lekkerkerker, J. Phys. Chem. B **105**, 10610 (2001).
[12] J. D. Parsons, Phys. Rev. A **19**, 1225 (1979).
[13] P. Sollich, P. B. Warren, and M. E. Cates, Adv. Chem. Phys. **116**, 265 (2001).
[14] N. Clarke, J. A. Cuesta, R. P. Sear, P. Sollich, and A. Speranza,

J. Chem. Phys. **113**, 5817 (2000).
[15] R. Zwanzig, J. Chem. Phys. **39**, 1714 (1963).
[16] In Onsager's original paper $\rho_{\mathrm{iso}} \equiv 1$ by construction. Here we adopt a slightly different definition for $\rho(l,l')$ [Eq. (5)] by retaining only the leading order term $2b$ of Eq. (6) instead of the full expression. This leads to $\rho_{\mathrm{iso}} = 1 + \mathcal{O}(L/D)$. Both definitions are equivalent up to leading order.
[17] I. S. Gradshteyn and I. M. Ryzhik, *Table of Integrals, Series and Products* (Academic Press, San Diego, 1994).
[18] G. J. Vroege and H. N. W. Lekkerkerker, Rep. Prog. Phys. **55**, 1241 (1992).
[19] D. Frenkel and B. M. Mulder, Mol. Phys. **55**, 1171 (1985).
[20] B. Tjipto-Margo and G. T. Evans, J. Chem. Phys. **94**, 4546 (1991).
[21] J. A. C. Veerman and D. Frenkel, Phys. Rev. A **45**, 5632 (1992).
[22] S. D. Lee, J. Chem. Phys. **87**, 4972 (1987).
[23] S. D. Lee, J. Chem. Phys. **89**, 7036 (1989).
[24] S. C. McGrother, D. C. Williamson, and G. Jackson, J. Chem. Phys. **104**, 6755 (1995).
[25] P. J. Camp, C. P. Mason, M. P. Allen, A. A. Khare, and D. A. Kofke, J. Chem. Phys. **105**, 2837 (1996).
[26] P. J. Camp and M. P. Allen, Physica A **229**, 410 (1996).
[27] P. J. Camp, M. P. Allen, P. G. Bolhuis, and D. Frenkel, J. Chem. Phys. **106**, 9270 (1997).
[28] B. Barboy and W. M. Gelbart, J. Chem. Phys. **71**, 3053 (1979).
[29] J. P. Hansen and I. R. McDonald, *Theory of Simple Liquids* (Academic Press, London, 1986).
[30] Note that these results only hold for Schulz-distributed parents within Parsons' rescaling approach. Different results might be obtained when adopting a different choice of Eq. (16) as a quantitative upgrade for the Onsager theory or a different parent distribution. However, our objective in this paper is to present a general framework allowing for arbitrary adaptations to be made with respect to these matters. A discussion of the effect of Parsons' approach on the isotropic-nematic transition densities can be found in Ref. [11].
[31] P. Sollich, J. Phys.; Condens. Matter **14**, R79 (2002).
[32] J. A. Cuesta, Europhys. Lett. **46**, 197 (1999).
[33] H. H. Wensink, G. J. Vroege, and H. N. W. Lekkerkerker (unpublished).